

Nonconvex Consensus ADMM for Cooperative Lane Change Maneuvers of Connected Automated Vehicles

Alexander Katriniok *

* *Ford Research & Innovation Center (RIC), Süsterfeldstr. 200,
52072 Aachen, Germany (e-mail: de.alexander.katriniok@ieee.org).*

Abstract: Connected and automated vehicles (CAVs) offer huge potential to improve the performance of automated vehicles (AVs) without communication capabilities, especially in situations when the vehicles (or agents) need to be cooperative to accomplish their maneuver. Lane change maneuvers in dense traffic, e.g., are very challenging for non-connected AVs. To alleviate this problem, we propose a holistic distributed lane change control scheme for CAVs which relies on vehicle-to-vehicle communication. The originally centralized optimal control problem is embedded into a consensus-based Alternating Direction Method of Multipliers framework to solve it in a distributed receding horizon fashion. Although agent dynamics render the underlying optimal control problem nonconvex, we propose a problem reformulation that allows to derive convergence guarantees. In the distributed setting, every agent needs to solve a nonlinear program (NLP) locally. To obtain a real-time solution of the local NLPs, we utilize the optimization engine **OpEn** which implements the proximal averaged Newton method for optimal control (PANOC). Simulation results prove the efficacy and real-time capability of our approach.

Keywords: Distributed control and estimation; Model predictive and optimization-based control; Real time optimization and control; Autonomous Vehicles; Multi-vehicle systems.

1. INTRODUCTION

Automated vehicles (AVs) usually take independent decisions which are based upon sensor measurements and motion predictions of surrounding vehicles. However, these predictions are often highly uncertain as they rely on simplified assumptions. This uncertainty may be crucial, especially in situations when the vehicles (hereafter referred to as *agents*) need to rely on these predicted trajectories to accomplish their maneuver. For instance, an AV might fail to perform a fully automated lane change or lane merging maneuver when traffic is dense and the target lane is already occupied. When exploiting vehicle-to-vehicle (V2V) communication, we can alleviate this issue by transmitting future control actions or state trajectories to other agents, or even by cooperatively negotiating control actions.

In this paper, we focus on fully automated lane change maneuvers in situations when the target lane is already occupied. During the last two decades, the problem of automating lane change maneuvers has intensively been discussed in literature, see Bevilacqua et al. (2016) for a comprehensive survey. In the recent years, cooperative control strategies have gained significant attention. Besides those based on consensus (Wang et al. (2017)) or lane change protocols (An and Jung (2018)), optimization based concepts are often a favorable choice as they allow to impose constraints and treat the control problem more holistically. Centralized schemes, which involve a central node that optimizes the agents' control actions, are discussed in Wang et al. (2016) and Hu and Sun (2019). Decentralized or distributed optimal control schemes, though, may be preferable as they are more resilient and scalable. Existing distributed schemes, such as Liu et al. (2017); Blasi et al. (2018), however, introduce conservatism to decouple the

agents or require the other agents' state space models to be known.

1.1 Main Contribution

We propose a distributed optimal control approach for collaborative, fully automated lane change maneuvers which adopts the consensus Alternating Direction Method of Multipliers (ADMM) (Bertsekas and Tsitsiklis (1989); Boyd et al. (2011)) as methodology to solve the lane change problem in a distributed receding horizon fashion. To exchange information, the agents rely on V2V communication. In the considered scenario, the *subject agent* (SA), i.e., the agent who intends to change lanes determines two consecutive agents in the target lane to eventually merge into the gap between them. The maneuver is then carried out in two steps: 1) the agents increase their headway distance to allow the SA to change lanes; 2) the SA changes lanes.

Compared to the literature, we aim to solve the originally centralized lane change problem in a distributed way without introducing additional conservatism. Particularly, every agent optimizes its local control actions while consensus with other agents is achieved through the use of a coordinator, which is run on the SA. As an advantage of our formulation, the agents' parameters and their state space models remain private and do not need to be known by the other agents. This way, we can also reduce load on the communication channel. Moreover, we holistically account for longitudinal and lateral vehicle motion instead of assuming the agents to change instantaneously from one lane to another. Essentially, every agent has to solve a nonconvex nonlinear program (NLP) while the coordinator problem is a standard quadratic program (QP). Although the local NLPs are nonconvex, we propose a problem

reformulation that allows to guarantee convergence of the nonconvex consensus ADMM problem. We run the algorithm in real-time by adopting **OpEn** (Optimization Engine) (Sopasakis et al. (2020)) which relies on the proximal averaged Newton method for optimal control (PANOC) (Stella et al. (2017)) to solve the local NLPs fast.

The remainder of the paper is organized as follows. First, we outline the lane change problem in Section 2. Then, we present a centralized formulation in Section 3 before we distribute the problem in Section 4. In Section 5, we discuss simulation results. Finally, we conclude and give an outlook for future work in Section 6.

1.2 Notation

With $x_{k+j|k}$, we refer to the prediction of variable x at the future time step $k+j$ given information up to time k while $x_{\cdot|k}$ denotes the trajectory of x along the entire prediction horizon of length $N \in \mathbb{N}_{>0}$. For $x \in \mathbb{R}^n$ and $i \in \{1, \dots, n\}$, x_i is the i -th entry of x , and the interval $[a, b] \subset \mathbb{N}$ with $a < b$ is denoted as $\mathbb{N}_{[a,b]}$. Finally, $[x]_+ \triangleq \max\{0, x\}$ for $x \in \mathbb{R}$ is referred to as the plus operator.

2. COOPERATIVE LANE CHANGE PROBLEM

2.1 Problem Description

Fig. 1 illustrates a sketch of the problem we intend to solve. To reduce complexity, we restrict ourselves to two lane scenarios, in which the SA wants to change lanes while the target lane is already occupied by other agents. This scheme, though, can easily be extended to scenarios with more than two lanes. In our use case, the SA sends a cooperation request to $N_A - 1$ agents in order to eventually merge in between two of these agents in the target lane. These are the preceding agent (PAT) and the following agent (FAT) in the target lane in accordance to Fig. 1. The preceding and following agent in the subject lane are referred to as PAS and FAS respectively.

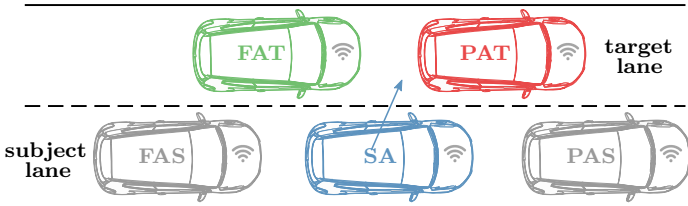


Fig. 1. Sketch of the lane change scenario with $N_A = 5$ cooperative agents. The SA (blue) aims to merge in between the PAT (red) and FAT (green).

Generally, the fully automated lane change maneuver can as such be subdivided into the following steps:

- (1) **Initialize cooperative group:** SA sets up a cooperative group of N_A agents, in which every agent can communicate with every other agent of the group.
- (2) **Negotiate agent order:** Determine PAT and FAT of SA in the target lane, i.e., the agents that will be in front and behind the SA after changing lanes.
- (3) **Establish headway:** There must be sufficient headway distance between PAT & FAT to let the SA in.
- (4) **Conduct lane change:** SA changes lanes.

Some of these steps may also be combined instead of solving them separately. To reduce complexity, we assume that Step 1 and Step 2 have already been accomplished, i.e., the PAT and FAT are known. These steps will further be investigated as part of future work. In this work, we propose a distributed algorithm to solve Step 3 and Step 4 while relying on the following fundamental assumptions.

Assumption 1. A1. All agents are equipped with V2V communication; A2. No communication failures or package dropouts occur; A3. Agent clocks are synchronized; A4. Every agent has access to a digital map to have knowledge about the road geometry ahead; A5. Every agent in the scenario belongs to the cooperative group.

Assumption A5 reduces complexity in the problem description but does not limit the applicability of our approach. Conversely, it can easily be extended in that direction.

2.2 Modeling

To derive a mathematical model of the lane change maneuver, a kinematic bicycle model (Rajamani (2012)) is adopted to describe the agents' motion in a curvilinear reference frame, see Fig. 2. For such kind of use case, it is a common approach in literature to apply the Frenet frame (Qian et al. (2016)), in which the agent's position is given in terms of its path coordinate s and the perpendicular displacement Δy from the road centerline. With this definition, the center of the subject lane in Fig. 1 is given by $(s, \Delta y) = (s, -w_{\text{lane}}/2)$ for any s where w_{lane} is the lane width. For every agent, we devise a state space model of the form

$$\dot{s} = v \cos(\Delta\psi + \beta) \left(\frac{1}{1 - \Delta y \kappa(s)} \right) \quad (1a)$$

$$\Delta\dot{y} = v \sin(\Delta\psi + \beta) \quad (1b)$$

$$\Delta\dot{\psi} = \frac{v}{l_r} \sin(\beta) - v \cos(\Delta\psi) \left(\frac{\kappa(s)}{1 - \Delta y \kappa(s)} \right) \quad (1c)$$

$$\dot{v} = a_x \quad (1d)$$

where

$$\beta = \arctan(\tan(\delta) l_r / (l_f + l_r))$$

denotes the vehicle sideslip angle, δ the wheel steering angle, v the vehicle speed, a_x the longitudinal vehicle acceleration, $\Delta\psi$ the heading error between the path tangent

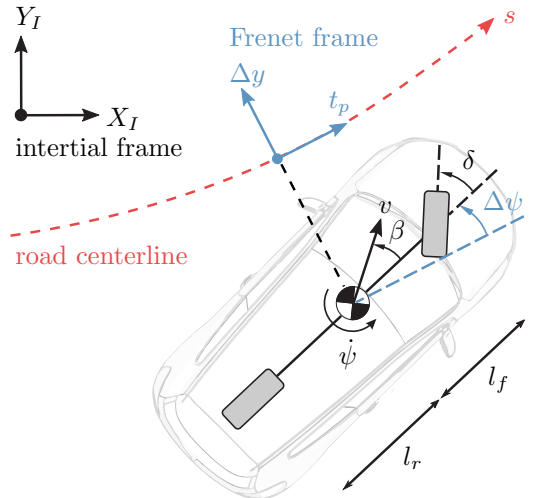


Fig. 2. Agent motion in the Frenet frame.

(along t_p) and the longitudinal vehicle axis. Moreover, l_f , l_r refer to the distance between the front respectively rear axle and the center of gravity. The path curvature $\kappa(s)$ of the road centerline is assumed to be a known parameterized curve (see assumption A4) in the path coordinate s .

The resulting nonlinear state space model $\dot{x} = f(x, u)$ features the state vector $x = [s, \Delta y, \Delta \psi, v]^\top \in \mathbb{R}^{n_x}$ and the input vector $u = [a_x, \delta]^\top \in \mathbb{R}^{n_u}$. It can be recognized that model (1) exhibits a singularity for $\Delta y = 1/\kappa(s) = r(s)$ where $r(s)$ is the path radius. In our case, though, even for a radius of 10m, a path deviation of 10m is very unlikely to happen. To subsequently differ between individual agents, we define the set of collaborative agents $\mathcal{A} \triangleq \{1, \dots, N_A\}$ where N_A is a positive integer. This way, we refer to the state vector x of agent $i \in \mathcal{A}$ as $x^{[i]}$.

3. CENTRALIZED FORMULATION

After generally introducing the cooperative lane change problem in Section 2.1, hereafter, we aim to formalize the problem in terms of an optimal control problem (OCP) which is solved in a receding horizon fashion. We start with a centralized formulation and derive its distributed variant in Section 4. Following Section 2.1, we subdivide the lane change in two maneuver steps.

(M-Step 1) SA, PAT & FAT establish required headway.

(M-Step 2) The SA changes lanes.

We integrate both steps in a single OCP as subsequently outlined.

Control Objectives To perform a proper fully automated cooperative lane change maneuver, the agents have to accommodate certain control objectives. First, every agent should track its reference speed v^{ref} (usually provided by a higher level planning algorithm). Second, the deviation from the lane center, defined through the desired lateral displacement Δy^{ref} from the road centerline, should be minimized. Additionally, we aim to minimize the heading error $\Delta \psi$ (thus choosing $\Delta \psi^{\text{ref}} = 0$) to reduce overshooting during a lane change. For reasons of comfort, we penalize the control input magnitude, that is, the applied longitudinal acceleration a_x and the wheel steering angle δ .

Along a horizon of N steps, we formalize these objectives for every agent $i \in \mathcal{A}$ as the stage cost at time $k+j$ for $j \in \mathbb{N}_{[0, N-1]}$

$$\ell_j^{[i]}(x_{k+j|k}^{[i]}, u_{k+j|k}^{[i]}) \triangleq u_{k+j|k}^{[i], \top} R^{[i]} u_{k+j|k}^{[i]} + (x_{k+j|k}^{[i]} - x_{k+j|k}^{[i], \text{ref}})^\top Q^{[i]} (x_{k+j|k}^{[i]} - x_{k+j|k}^{[i], \text{ref}}) \quad (2)$$

and the terminal cost

$$\ell_N^{[i]}(x_{k+N|k}^{[i]}) \triangleq (x_{k+N|k}^{[i]} - x_{k+N|k}^{[i], \text{ref}})^\top Q_N^{[i]} (x_{k+N|k}^{[i]} - x_{k+N|k}^{[i], \text{ref}}) \quad (3)$$

where $x_{k+j|k}^{[i], \text{ref}} \triangleq [s_{k+j|k}^{[i], \text{ref}}, \Delta y_{k+j|k}^{[i], \text{ref}}, \Delta \psi_{k+j|k}^{[i], \text{ref}}, v_{k+j|k}^{[i], \text{ref}}]^\top$ denotes the reference state while $Q^{[i]} \triangleq \text{diag}(q_s^{[i]}, q_{\Delta y}^{[i]}, q_{\Delta \psi}^{[i]}, q_v^{[i]}) \succeq 0$, $Q_N^{[i]} \triangleq \text{diag}(q_{N,s}^{[i]}, q_{N,\Delta y}^{[i]}, q_{N,\Delta \psi}^{[i]}, q_{N,v}^{[i]}) \succeq 0$ and $R^{[i]} \triangleq \text{diag}(r_{a_x}^{[i]}, r_{\delta}^{[i]}) \succ 0$ are positive (semi)definite weighting matrices.

Constraints Besides control objectives, we need to ensure that agents only move in their designated lanes. Thus, we constrain the lateral displacement Δy . Moreover, the agents should not exceed the maximum speed $\bar{v}_{k+j|k}^{[i]}$ at time $k+j$ and not drive backwards. That said, we are able to derive the admissible state set

$$\mathcal{X}_{k+j|k}^{[i]} \triangleq \left\{ x \in \mathbb{R}^{n_x} \mid \Delta y_{k+j|k}^{[i]} \leq x_2 \leq \Delta \bar{y}_{k+j|k}^{[i]} \right. \\ \left. \wedge 0 \leq x_4 \leq \bar{v}_{k+j|k}^{[i]} \right\} \quad (4)$$

at time $k+j$ for $j \in \mathbb{N}_{[1, N]}$ where $\Delta y_{k+j|k}^{[i]}$ and $\Delta \bar{y}_{k+j|k}^{[i]}$ are reasonable bounds which assure that agents in neighboring lanes have a minimum lateral distance to each other. Due to actuator limitations and for reasons of ride comfort and vehicle stability, we constrain the control actions by

$$\mathcal{U}^{[i]} \triangleq \{ u \in \mathbb{R}^{n_u} \mid \underline{a}_x \leq u_1 \leq \bar{a}_x \wedge \underline{\delta} \leq u_2 \leq \bar{\delta} \} \quad (5)$$

where \underline{a}_x , \bar{a}_x and $\underline{\delta}$, $\bar{\delta}$ are appropriately chosen lower and upper bounds respectively. Moreover, for the same reason, we bound the lateral acceleration (i.e., the product of longitudinal velocity and yaw rate)

$$a_y^{[i]} = (v^{[i]} \cos(\beta^{[i]})) \cdot (v^{[i]} \sin(\beta^{[i]})) / l_r^{[i]}$$

and the total acceleration $a_{\text{tot}}^{[i]} = ((a_x^{[i]})^2 + (a_y^{[i]})^2)^{1/2}$ through the constraints

$$-\bar{a}_y^{[i]} \leq a_{y,k+j|k}^{[i]} \leq \bar{a}_y^{[i]} \wedge (a_{\text{tot},k+j|k}^{[i]})^2 \leq (\bar{a}_{\text{tot}}^{[i]})^2, \quad (6)$$

as a function of $(u_{k+j|k}^{[i]}, x_{k+j|k}^{[i]})$, for $j \in \mathbb{N}_{[0, N-1]}$ with appropriate upper bounds $\bar{a}_y^{[i]} > 0$ and $\bar{a}_{\text{tot}}^{[i]} > 0$.

Let $\text{Pd}(i) \subset \mathcal{A}$ denote the set of preceding vehicles of Agent i . In case Agent i is the SA, $\text{Pd}(i)$ contains the PAT and, until M-Step 2 is completed, the PAS. If Agent i is the FAT, $\text{Pd}(i)$ contains the SA and, until M-Step 2 is completed, the PAT. For all other agents, $\text{Pd}(i)$ is the agent that is physically ahead. To establish the headway distance between SA, PAT and FAT (M-Step 1) and to avoid collisions between agents, Agent i bounds the headway distance from below, i.e.,

$$s_{k+j|k}^{[i]} - s_{k+j|k}^{[l]} \geq d_{\text{hw}}, \quad \forall l \in \text{Pd}(i) \quad (7)$$

where the lower bound $d_{\text{hw}} > 0$ also encodes the vehicles' geometry. As the agents' path coordinate s refers to the road centerline (see Section 2.2), d_{hw} has additionally to be increased on highly curved road sections in dependence of the (maximum) road curvature $|\kappa(s)|$.

Optimization Problem For notational convenience, hereafter, we stack the states of all agents $i \in \mathcal{A}$ at time $k+j$ in a single vector, i.e., $\bar{x}_{k+j|k} \triangleq (x_{k+j|k}^{[i]})_{i=1}^{N_A}$. Likewise, for the control inputs, we define $\bar{u}_{k+j|k} \triangleq (u_{k+j|k}^{[i]})_{i=1}^{N_A}$. Additionally, when referring to the entire state or input trajectory, we write $\bar{x}_{\cdot|k} \triangleq (\bar{x}_{k+j|k})_{j=1}^N$ and $\bar{u}_{\cdot|k} \triangleq (\bar{u}_{k+j|k})_{j=0}^{N-1}$. This way, we introduce the aggregated stage costs

$$\ell_N(\bar{x}_{k+N|k}) \triangleq \sum_{i=1}^{N_A} \ell_N^{[i]}(x_{k+N|k}^{[i]}), \\ \ell_j(\bar{x}_{k+j|k}, \bar{u}_{k+j|k}) \triangleq \sum_{i=1}^{N_A} \ell_j^{[i]}(x_{k+j|k}^{[i]}, u_{k+j|k}^{[i]}).$$

By adopting a direct multiple shooting formulation (Bock and Plitt (1984)), that is, including the discrete-time

system dynamics as equality constraints in the OCP, we phrase the resulting **centralized lane change NLP** as

$$\underset{\bar{u}_{\cdot|k}, \bar{x}_{\cdot|k}}{\text{minimize}} \quad \ell_N(\bar{x}_{k+N|k}) + \sum_{j=0}^{N-1} \ell_j(\bar{x}_{k+j|k}, \bar{u}_{k+j|k}) \quad (8a)$$

s.t. for every agent $i \in \mathcal{A}$:

$$u_{k+j|k}^{[i]} \in \mathcal{U}^{[i]}, \quad j \in \mathbb{N}_{[0, N-1]} \quad (8b)$$

$$x_{k+j|k}^{[i]} \in \mathcal{X}_{k+j|k}^{[i]}, \quad j \in \mathbb{N}_{[1, N]} \quad (8c)$$

$$x_{k+j+1|k}^{[i]} = f_d^{[i]}(x_{k+j|k}^{[i]}, u_{k+j|k}^{[i]}), \quad j \in \mathbb{N}_{[0, N-1]} \quad (8d)$$

$$-\bar{a}_y^{[i]} \leq a_{y, k+j|k}^{[i]} \leq \bar{a}_y^{[i]}, \quad j \in \mathbb{N}_{[0, N-1]} \quad (8e)$$

$$(a_{\text{tot}, k+j|k}^{[i]})^2 \leq (\bar{a}_{\text{tot}}^{[i]})^2, \quad j \in \mathbb{N}_{[0, N-1]} \quad (8f)$$

$$s_{k+j|k}^{[l]} - s_{k+j|k}^{[i]} \geq d_{\text{hw}}, \quad \forall l \in \text{Pd}(i); j \in \mathbb{N}_{[1, N]} \quad (8g)$$

$$x_{k|k}^{[i]} = x_k^{[i]}, \quad (8h)$$

where

$$f_d^{[i]}(x_{k+j|k}^{[i]}, u_{k+j|k}^{[i]}) \triangleq x_{k+j|k}^{[i]} + \int_{t_{k+j}}^{t_{k+j+1}} f(x^{[i]}(\tau), u_{k+j|k}^{[i]}) d\tau \quad (9)$$

represents the discretized system dynamics using zero order hold. We approximate the integral in (9) using a 4th order Runge-Kutta method (Nocedal and Wright (2006)).

Remark 1. During M-Step 1, the SA's reference value Δy^{ref} is set to the center of the subject lane while the bounds on Δy prevent the SA from leaving its lane. When the required headway distance between the SA, PAT and FAT has been established (for time t_k and the entire prediction horizon), the bounds on Δy are modified in M-Step 2 to allow the SA to drive in both lanes. Simultaneously, the reference Δy^{ref} is set to the center of the target lane to initiate the lane change. After M-Step 2, the bounds on Δy are finally adapted to the target lane.

4. DISTRIBUTED SOLUTION USING ADMM

Compared to a centralized formulation, as described in Section 3, distributing computations among the agents appears to be more scalable and resilient. For a distributed control scheme that could eventually be implemented in a test vehicle, we impose the following requirements.

Requirements 1. R1. The agents' state space models and their parameters should be private; R2. Instead of the entire state vector, only position information should be exchanged to reduce communication load; R3. The distributed OCP must be solved within the sampling time, including the time for data exchange via V2V.

To solve Problem (8) in a distributed fashion, we apply the consensus Alternating Direction Method of Multipliers (ADMM) (Bertsekas and Tsitsiklis (1989)). As shown in the remainder of this section, we decompose Problem (8) such that objectives and constraints, belonging to the individual agent, are incorporated in a local OCP while the joint satisfaction of the minimum headway distance is tackled by a coordinator which is run on the SA.

4.1 Problem Reformulation and Decomposition

To come up with a distributed OCP that is compliant with a consensus ADMM formulation, in a first step, we need

to reformulate Problem (8). For notational convenience, we define an augmented optimization vector that contains control input and state trajectories over the prediction horizon, that is, $\xi_{\cdot|k}^{[i]} = (x_{k+j|k}^{[i]}, u_{k+j-1|k}^{[i]})_{j=1}^N$. Moreover, the aggregated vector $\bar{\xi}_{\cdot|k} \triangleq (\xi_{\cdot|k}^{[i]})_{i=1}^{N_A}$ stacks the variables $\xi_{\cdot|k}^{[i]}$ for every agent $i \in \mathcal{A}$ in a single vector. This way, we can summarize equality constraints (8d) in a compact form as $h^{[i]}(\xi_{\cdot|k}^{[i]}) = 0$. Likewise, inequality constraints (8e) and (8f) can concisely be stated as $g^{[i]}(\xi_{\cdot|k}^{[i]}) \leq 0$. That said, we introduce the associated indicator functions

$$\mathbb{1}_{h^{[i]}}(\xi_{\cdot|k}^{[i]}) \triangleq \begin{cases} 0, & h^{[i]}(\xi_{\cdot|k}^{[i]}) = 0 \\ \infty, & \text{otherwise,} \end{cases} \quad (10)$$

$$\mathbb{1}_{g^{[i]}}(\xi_{\cdot|k}^{[i]}) \triangleq \begin{cases} 0, & g^{[i]}(\xi_{\cdot|k}^{[i]}) \leq 0 \\ \infty, & \text{otherwise.} \end{cases} \quad (11)$$

To accommodate equality and inequality constraints, we define the augment cost for every agent i as

$$\phi^{[i]}(\xi_{\cdot|k}^{[i]}) \triangleq \ell_N^{[i]}(x_{k+N|k}^{[i]}) + \sum_{j=0}^{N-1} \ell_j^{[i]}(x_{k+j|k}^{[i]}, u_{k+j|k}^{[i]}) + \mathbb{1}_{h^{[i]}}(\xi_{\cdot|k}^{[i]}) + \mathbb{1}_{g^{[i]}}(\xi_{\cdot|k}^{[i]}). \quad (12)$$

Moreover, we define a cost associated with the minimum headway distance constraints (8g), i.e.,

$$\gamma(\bar{\xi}_{\cdot|k}) \triangleq \sum_{j=1}^N \sum_{i=1}^{N_A} \sum_{l \in \text{Pd}(i)} \mathbb{1}_{\text{hw}}(\xi_{k+j|k}^{[i]}, \xi_{k+j|k}^{[l]}) \quad (13)$$

with the indicator function

$$\mathbb{1}_{\text{hw}}(\xi_{k+j|k}^{[i]}, \xi_{k+j|k}^{[l]}) \triangleq \begin{cases} 0, & s_{k+j|k}^{[l]} - s_{k+j|k}^{[i]} \geq d_{\text{hw}} \\ \infty, & \text{otherwise.} \end{cases}$$

As the minimum headway distance constraints are convex, so is the associated indicator function $\mathbb{1}_{\text{hw}}$ and as such the cost γ . With (12) and (13), we can rewrite the centralized NLP (8) as a **box constrained NLP**

$$\underset{\bar{\xi}_{\cdot|k}}{\text{minimize}} \quad \gamma(\bar{\xi}_{\cdot|k}) + \sum_{i=1}^{N_A} \phi^{[i]}(\xi_{\cdot|k}^{[i]}) \quad (14a)$$

$$\text{s.t.} \quad \xi_{k+j|k}^{[i]} \in \Xi_{k+j|k}^{[i]}, \quad i \in \mathcal{A}, j \in \mathbb{N}_{[1, N]} \quad (14b)$$

where the original input and state constraints (8b) and (8c) are represented by the close and convex feasible set

$$\Xi_{k+j|k}^{[i]} \triangleq \left\{ (x_{k+j|k}^{[i]}, u_{k+j-1|k}^{[i]}) \in (\mathcal{X}_{k+j|k}^{[i]} \times \mathcal{U}^{[i]}) \subseteq \mathbb{R}^{n_x} \times \mathbb{R}^{n_u} \right\}.$$

To decouple the agents, we introduce new auxiliary variables $z_{\cdot|k}^{[i]} \triangleq (z_{k+j|k}^{[i]})_{j=1}^N$ respectively $\bar{z}_{\cdot|k} \triangleq (z_{\cdot|k}^{[i]})_{i=1}^{N_A}$ which correspond to Agent i 's path coordinate $s^{[i]}$ over the prediction horizon. By imposing the *consensus constraint* $c_{\text{cc}}^\top \xi_{k+j|k}^{[i]} = z_{k+j|k}^{[i]}$ with $c_{\text{cc}} \triangleq [1 \ 0 \ 0 \ 0 \ 0 \ 0]^\top$ for every $j \in \mathbb{N}_{[1, N]}$ and every agent $i \in \mathcal{A}$, we can rewrite (14) as an **equivalent problem with auxiliary variables**

$$\underset{\bar{\xi}_{\cdot|k}, \bar{z}_{\cdot|k}}{\text{minimize}} \quad \gamma(\bar{z}_{\cdot|k}) + \sum_{i=1}^{N_A} \phi^{[i]}(\xi_{\cdot|k}^{[i]}) \quad (15a)$$

$$\text{s.t.} \quad c_{\text{cc}}^\top \xi_{k+j|k}^{[i]} = z_{k+j|k}^{[i]}, \quad i \in \mathcal{A}, j \in \mathbb{N}_{[1, N]} \quad (15b)$$

$$\xi_{k+j|k}^{[i]} \in \Xi_{k+j|k}^{[i]}, \quad i \in \mathcal{A}, j \in \mathbb{N}_{[1, N]} \quad (15c)$$

By virtue of Problem (15), it can be recognized that the agents' cost $\phi^{[i]}$ solely depends on the local optimization variable $\xi_{\cdot|k}^{[i]}$. Conversely, the cost γ , which accommodates the minimum headway distance constraints, relies on the auxiliary variables $z_{\cdot|k}^{[i]}$ or *copies* of the agents' path coordinate $s^{[i]}$ over the prediction horizon. Such formulation motivates a distributed solution of Problem (15), that is, every agents optimizes its local OCP while the minimum headway distance constraints are accommodated by a coordinator. For reasons of brevity, hereafter, we abbreviate constraint (15b) as $C_{cc}\xi_{\cdot|k}^{[i]} = z_{\cdot|k}^{[i]}$ where C_{cc} is a matrix of appropriate dimension.

Remark 2. Our choice of c_{cc} in (15b) is crucial to satisfy requirements R1 and R2. This way, only the agents' path coordinates $s^{[i]} = c_{cc}^\top \xi_{\cdot|k}^{[i]}$ need to be exchanged amongst each other via V2V.

4.2 Consensus ADMM Framework

To embed the reformulated Problem (15) in the ADMM framework, we *dualize* consensus constraint (15b) and obtain the Augmented Lagrangian function (Bertsekas and Tsitsiklis (1989))

$$\mathcal{L}_\rho(\bar{\xi}_{\cdot|k}, \bar{z}_{\cdot|k}, \bar{\lambda}) = \gamma(\bar{z}_{\cdot|k}) + \sum_{i=1}^{N_A} \phi^{[i]}(\xi_{\cdot|k}^{[i]}) + \sum_{i=1}^{N_A} \left[(\lambda^{[i]})^\top (C_{cc}\xi_{\cdot|k}^{[i]} - z_{\cdot|k}^{[i]}) + \frac{\rho}{2} \|C_{cc}\xi_{\cdot|k}^{[i]} - z_{\cdot|k}^{[i]}\|^2 \right] \quad (16)$$

where $\rho > 0$ is a constant penalty parameter, $\lambda^{[i]}$ is the vector of Lagrangian multipliers associated with consensus constraint (15b), and $\bar{\lambda} \triangleq (\lambda^{[i]})_{i=1}^{N_A}$ is the aggregated vector of multipliers. The consensus ADMM algorithm, applied to minimize (16) subject to $\xi_{k+j|k}^{[i]} \in \Xi_{k+j|k}^{[i]}$ for $i \in \mathcal{A}$ and $j \in \mathbb{N}_{[1,N]}$, is summarized in Algorithm 1. In a receding horizon fashion, we run the following steps at time k .

Step 1: Starting with an initial guess $(\xi_{\cdot|k}^{[i]}, z_{\cdot|k}^{[i]}, \lambda^{[i]})$, every agent solves the box constrained NLP (18) and transmits the optimized path coordinate trajectory $s_{\cdot|k}^{[i]} = C_{cc}\xi_{\cdot|k}^{[i]}$ to the coordinator. As $\phi^{[i]}$ in (16) is nonsmooth and nonconvex, NLP (18) adopts a smooth but still nonconvex reformulation $\Phi^{[i]}$ to guarantee convergence of the ADMM scheme, see Section 4.3 and Section 4.4.

Step 2: The coordinator (residing on the SA) solves the constrained coordination QP (19) which imposes the minimum headway distance (encoded in γ) as linear constraints (cf. (8g)). For notational convenience, we abbreviate this constraint as $\bar{C}_{hw}\bar{z}_{\cdot|k} \leq \bar{d}_{hw}$ where \bar{C}_{hw} and \bar{d}_{hw} are a matrix and a vector of appropriate dimension. Mostly, the initial condition of the lane change maneuver may look like in Fig. 1. Then, the original constraint (8g) may not be satisfied. As a consequence, we may not be able to establish consensus without either violating agent dynamics (as we would need to shift agents' positions instantaneously to satisfy (8g)) or the minimum headway distance constraints. For this reason, we reformulate the minimum headway distance constraint as a soft constraint

$$\bar{C}_{hw}\bar{z}_{\cdot|k} \leq \bar{d}_{hw} + \bar{E}_{hw}\epsilon \quad \text{with } \epsilon \triangleq (\epsilon_{i,l})_{i \in \mathcal{A}, l \in \text{Pd}(i)} \quad (17)$$

Algorithm 1 Nonconvex ADMM Problem at time k

Initial guess: $\bar{\xi}_{\cdot|k}, \bar{z}_{\cdot|k}, \bar{\lambda}$ (every agent & coordinator)
repeat

1) **Every agent** $i \in \mathcal{A}$: Solve NLP in parallel

$$\xi_{\cdot|k}^{[i]} \leftarrow \arg \min_{\xi_{\cdot|k}^{[i]}} \Phi^{[i]}(\xi_{\cdot|k}^{[i]}; \alpha, \mu) + (\lambda^{[i]})^\top C_{cc}\xi_{\cdot|k}^{[i]} + \frac{\rho}{2} \|C_{cc}\xi_{\cdot|k}^{[i]} - z_{\cdot|k}^{[i]}\|^2 \quad (18)$$

$$\text{s.t. } \xi_{\cdot|k}^{[i]} \in \Xi_{\cdot|k}^{[i]}$$

and transmit $C_{cc}\xi_{\cdot|k}^{[i]}$ to coordinator.

2) **Coordinator:** Solve coordination QP

$$\bar{z}_{\cdot|k} \leftarrow \arg \min_{\bar{z}_{\cdot|k}, \epsilon} \sum_{i=1}^{N_A} \left[-(\lambda^{[i]})^\top z_{\cdot|k}^{[i]} + \frac{\rho}{2} \|C_{cc}\xi_{\cdot|k}^{[i]} - z_{\cdot|k}^{[i]}\|^2 \right] + q_\epsilon^\top \epsilon \quad (19)$$

$$\text{s.t. } \bar{C}_{hw}\bar{z}_{\cdot|k} \leq \bar{d}_{hw} + \bar{E}_{hw}\epsilon, \quad \epsilon_{i,l} \geq 0.$$

3) **Coordinator:** Perform dual gradient step

$$\lambda^{[i]} \leftarrow \lambda^{[i]} + \rho (C_{cc}\xi_{\cdot|k}^{[i]} - z_{\cdot|k}^{[i]}), \quad \forall i \in \mathcal{A}. \quad (20)$$

4) **Coordinator:** Broadcast $(\bar{\lambda}, \bar{z}_{\cdot|k})$ to every agent.

until stopping criterion satisfied

where ϵ is a vector of slack variables $\epsilon_{i,l} \geq 0$ for every (i, l) with $i \in \mathcal{A}$ and $l \in \text{Pd}(i)$ and \bar{E}_{hw} is a matrix of appropriate dimension. That way, consensus can be established and $\epsilon_{i,l} \rightarrow 0$ will hold after M-Step 1 is completed. Moreover, we augment the cost function in QP (19) with the additional linear cost term $q_\epsilon^\top \epsilon \geq 0$ that penalizes ϵ where q_ϵ is a weighting vector of appropriate dimension with all weights larger than zero. The resulting Problem (19) is a standard QP that optimizes over $(\bar{z}_{\cdot|k}, \epsilon)$. Its solution can be obtained fast using mature QP solvers.

Step 3 & 4: The coordinator updates the dual variables $\lambda^{[i]}$ and transmits the vectors $(\bar{\lambda}, \bar{z}_{\cdot|k})$ to the agents.

This scheme is iterated until the stopping criteria, adopted from (Boyd et al., 2011, Sec. 3.1.1), is satisfied, that is, until the norm of the primal and dual residuals are below their thresholds $\epsilon^{\text{prim}} \geq 0$ and $\epsilon^{\text{dual}} \geq 0$ respectively

$$\|\xi_{\cdot|k} - \bar{z}_{\cdot|k}\| \leq \epsilon^{\text{prim}}, \quad \|(\rho [C_{cc}\xi_{\cdot|k}^{[i]} - z_{\cdot|k}^{[i]}])_{i=1}^{N_A}\| \leq \epsilon^{\text{dual}}. \quad (21)$$

After convergence, every agent i applies the control action $u_{k|k}^{[i]*}$ locally. At the next time step $k+1$, Algorithm 1 is warm-started by exploiting the solution $(\bar{\xi}_{\cdot|k}^*, \bar{z}_{\cdot|k}^*, \bar{\lambda}^*)$ from time step k as initial guess.

4.3 Agent NLPs: Smooth Reformulation and Solution

To ensure convergence of Algorithm 1, $\phi^{[i]}$ in (16) needs to be convex or at least a smooth nonconvex function, see Hong et al. (2016). Convexity, though, is not satisfied due to nonconvex system dynamics $h^{[i]}(\xi_{k+j|k}^{[i]}) = 0$. At the same time, indicator functions in (12) are nonsmooth. Therefore, we come up with a smooth reformulation of the indicator functions $\mathbb{1}_{h^{[i]}}$ and $\mathbb{1}_{g^{[i]}}$.

By applying the Augmented Lagrangian method (ALM) (Nocedal and Wright, 2006, Chap. 17), we replace the indicator function $\mathbb{1}_{h^{[i]}(\xi_{\cdot|k}^{[i]})}$ of the equality constraints, related to system dynamics, with the cost

$$\phi_{\text{ALM}}(\xi_{\cdot|k}^{[i]}; \alpha, \mu) \triangleq \mu^\top h^{[i]}(\xi_{\cdot|k}^{[i]}) + \frac{\alpha}{2} \|h^{[i]}(\xi_{\cdot|k}^{[i]})\|^2 \quad (22)$$

where $\alpha > 0$ is a penalty parameter and μ the vector of Lagrangian multipliers related to the equality constraints. Moreover, we rephrase inequality constraints $g^{[i]}(\xi_{\cdot|k}^{[i]}) \leq 0$ as equality constraints $G(\xi_{\cdot|k}^{[i]}) = 0$ (Sopasakis et al. (2020)) where for each constraint $\iota = 1, \dots, n_{\text{ineq}}$ holds

$$G_\iota(\xi_{\cdot|k}^{[i]}) \triangleq [g_\iota^{[i]}(\xi_{\cdot|k}^{[i]})]_+. \quad (23)$$

As (23) is a nonsmooth function, we can not formulate $G(\xi_{\cdot|k}^{[i]}) = 0$ as an ALM-type constraint (Sopasakis et al. (2020)). Instead, we apply the quadratic penalty method (PM) (Nocedal and Wright, 2006, Chap. 17) to replace the indicator function (11) of the inequality constraints with the cost

$$\phi_{\text{PM}}(\xi_{\cdot|k}^{[i]}; \alpha) \triangleq \frac{\alpha}{2} \|G(\xi_{\cdot|k}^{[i]})\|^2. \quad (24)$$

With (22) and (24), we gain the Augmented Lagrangian function of the local OCP

$$\Phi^{[i]}(\xi_{\cdot|k}^{[i]}; \alpha, \mu) \triangleq \phi^{[i]}(\xi_{\cdot|k}^{[i]}) + \phi_{\text{ALM}}(\xi_{\cdot|k}^{[i]}; \alpha, \mu) + \phi_{\text{PM}}(\xi_{\cdot|k}^{[i]}; \alpha)$$

which is a nonconvex \mathcal{C}^1 continuous differentiable function and as such a smooth reformulation of $\phi^{[i]}$. To compute a local solution of NLP (18), we apply the open source code framework `OpEn v0.6.2` (Sopasakis et al. (2020)), available on github.com/alphaville/optimization-engine. In an inner loop, `OpEn` utilizes the proximal averaged Newton method for optimal control (PANOC) to solve NLP (18) for a fixed penalty α and fixed Lagrangian multipliers μ . In an outer loop, α and μ are updated to achieve constraint satisfaction as described in Sopasakis et al. (2020). In every iteration of Algorithm 1 at time step k , the solver is warm-started with the solution of the previous iteration. Likewise, `OpEn` is warm-started at time step $k+1$ by exploiting the solution from time step k . For such kind of problems, PANOC has already shown superior performance (Stella et al. (2017); Katriniok et al. (2019)).

4.4 Convergence

For convex consensus ADMM problems, that is, if every $\phi^{[i]}$ and γ in (15) are convex, convergence has been proven in literature (Boyd et al. (2011)). For nonconvex functions $\phi^{[i]}$ respectively $\Phi^{[i]}$, as in our case, we can show that the nonconvex consensus ADMM problem as well as the subproblems (18) converge to a set of stationary points under some mild conditions (Hong et al. (2016); Wang et al. (2019); Sopasakis et al. (2020)). Without any assumptions on the iterates, Algorithm 1 is guaranteed to converge to a set of stationary points (i.e., to a local solution) if Problem (15) meets certain regularity conditions and the step size ρ is chosen large enough. By virtue of Hong et al. (2016), our problem satisfies all assumptions which are a prerequisite to convergence, such as: the feasible set $(\Xi_{k+j|k}^{[i]})_{i \in \mathcal{A}, j \in \mathbb{N}_{[1, N]}}$ is closed and convex, γ is convex and $\Phi^{[i]}$ has a Lipschitz-continuous gradient if the steering angle δ is constrained on the interval $(-\pi/2, \pi/2)$ — technically, even tighter bounds are required, see Section 5.1.

5. SIMULATION RESULTS

5.1 Simulation Setup

For a proof of concept, we evaluate the proposed consensus ADMM-based framework in a realistic lane change scenario with $N_A = 3$ cooperative connected agents. According to Fig. 5a, the SA (Agent 2, blue) is driving on the right (subject) lane while the PAT (Agent 1, red) and FAT (Agent 3, green) on the left (target) lane are initially blocking the road for a lane change of the SA.

In the simulation study, we adopt the control-oriented model (1) as validation model. Every agent has dimensions $L^{[i]} = 5$ m, $W^{[i]} = 2$ m, $l_f^{[i]} = 1.4$ m and $l_r^{[i]} = 1.4$ m. The distance between the center of gravity and the front respectively rear bumper is 2.5 m. In our scenario, we want the agents to keep a bumper-to-bumper distance of 10 m. Taking vehicle dimensions and road curvature into account (the road radius is always larger or equal to 200 m), we set d_{hw} to 15 m. This way, the minimum bumper-to-bumper distance is approximately 10 m. For every agent, the initial and reference velocity is set to 14 m/s. With a lane width of $w_{\text{lane}} = 4$ m, the initial Frenet coordinates $(s^{[i]}, \Delta y^{[i]})$ are (12 m, 2 m) and (0 m, 2 m) for the PAT (red) and FAT (green) in the left lane, respectively, while the initial coordinates of the SA (blue) in the right lane are (6 m, -2 m), see Fig. 5a.

In the consensus ADMM framework, we have selected the same weights for every agent: $q_s^{[i]} = 0$, $q_{\Delta y}^{[i]} = 1$, $q_{\Delta \psi}^{[i]} = 100$, $q_v^{[i]} = 1$, $r_{a_x}^{[i]} = 1$, $r_{\delta}^{[i]} = 600$ and $Q_N^{[i]} = Q^{[i]}$. The sample period between two consecutive runs of Algorithm 1 is set to $T_s = 0.1$ s, the horizon length to $N = 15$ and the penalty parameter to $\rho = 100$. To keep the agents in their designated lanes, the bounds $(\Delta y^{[i]}, \Delta \bar{y}^{[i]})$ on the lateral displacement are chosen as (1.25 m, 2.75 m) for the left lane and (-1.25 m, -2.75 m) for the right lane. The absolute longitudinal acceleration should always be less or equal to 4 m/s², the absolute lateral acceleration should not exceed 3.5 m/s² and the total acceleration is bounded from above by 4 m/s². Finally, the steering angle should be within ± 5 deg while the maximum velocity is set to 17 m/s. Simulations are run on an Intel i7 machine at 2.9 GHz with Matlab R2018b.

5.2 Discussion of Results

In Fig. 3, we illustrate the optimized state and input trajectories of the three agents while the steering angle plot (bottom plot, Fig. 3) is augmented with the SA's lateral acceleration and its upper bound. Moreover, Fig. 5 highlights three snapshots of the lane change maneuver.

During M-Step 1 of the maneuver, that is, until $t = 4.7$ s (light orange patch in Fig. 3, 1st plot) the agents establish the required headway distance to allow the SA (blue) to change lanes safely. As a minimum cost maneuver, the PAT (red) accelerates and the FAT (green) decelerates to increase the headway distance whereas the SA (blue) keeps its speed almost constant. As the SA (blue) is located in the middle of the PAT (red) and FAT (green), the acceleration and speed trajectories of PAT and FAT are symmetric to each other — which appears to be the most

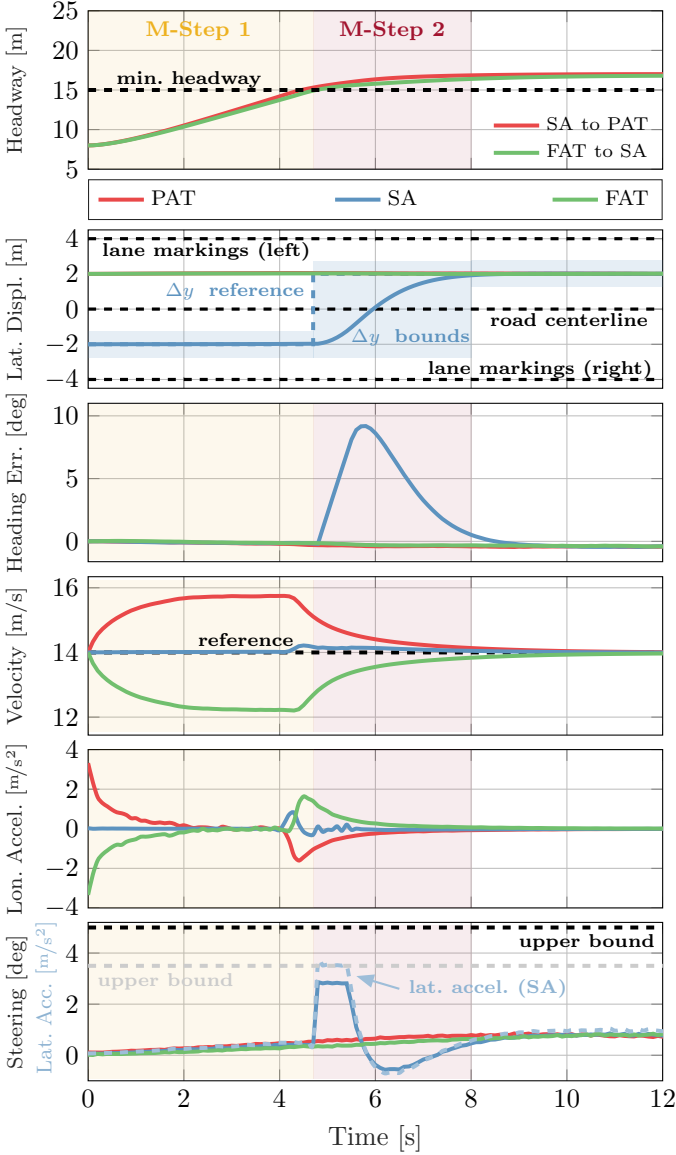


Fig. 3. Optimized state and input trajectories of the lane change maneuver. M-Step 1 is accomplished at $t = 4.7$ s and M-Step 2 at $t = 8.0$ s.

reasonable cooperative maneuver. The maximum absolute longitudinal acceleration during M-Step 1 is 3.3 m/s^2 .

At the beginning of M-Step 2 (light purple patch in Fig. 3, 1st plot), the SA (blue) modifies its reference value Δy^{ref} (dashed blue line in Fig. 3, 2nd plot) from -2 m (right lane) to 2 m (left lane). At the same time, the constraint bounds on the lateral displacement are adjusted to $(\Delta y^{[i]}, \Delta \bar{y}^{[i]}) = (-2.75 \text{ m}, 2.75 \text{ m})$, see blue patch in Fig. 3, 2nd plot. This enables the SA (blue) to drive in both lanes and to initiate the lane change, see Fig. 5b. The lane change maneuver is accomplished after 3.3 s, that is, at $t = 8 \text{ s}$, see also Fig. 5c. As we are rather focusing on lane change maneuvers than on platooning, there is no need to bound the headway distance from above to obtain a high vehicle density in the target lane. Consequently, the headway distance between the SA (blue) and the PAT (red) is always larger than the lower bound of 15 m .

Right after the end of M-Step 2, the agents' speed trajectory converge to the common set point of 14 m/s . As the

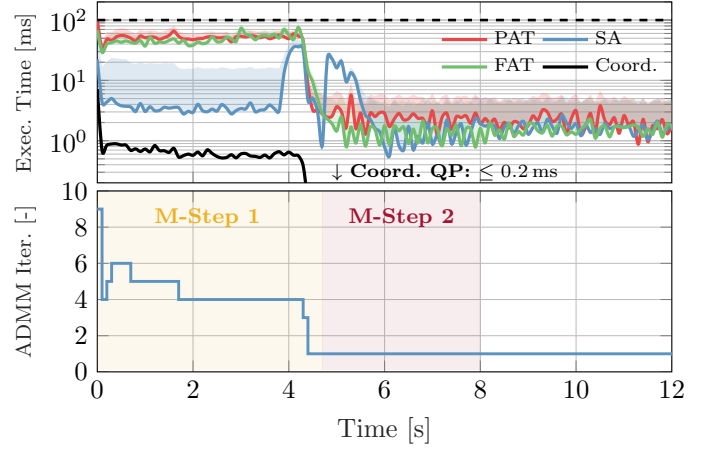


Fig. 4. Execution times (top) for solving the OCPs (solid lines) as a sum over all ADMM iterations (bottom) along with communication overhead (shaded area). The solving time of the coordination QP has been added to the SA communication overhead (blue shaded area).

maneuver is performed on a curved road, the wheel steering angle is almost always different from zero. During the entire maneuver, the agents' state and input trajectories are always smooth and within their designated bounds — thus, satisfying all our requirements.

Finally, the real-time capability of proposed control scheme, according to requirement R3 (see Section 4), needs to be assessed. Fig. 4 provides an overview of the agents' and the coordinator's execution times (top) and the required ADMM iterations (bottom). The execution times include the time needed to solve the local NLPs (solid lines in top plot) as well as the communication overhead related to the ADMM iterations (shaded area in same color, top plot). For the SA (blue), the shaded area additionally incorporates the solving time of the coordination QP. As communication overhead, we assume a maximum end-to-end latency of 3 ms as it has been specified by the 3rd Generation Partnership Project (3GPP) for the new 5G communication standard in order to support advanced driving functions (3GPP.org (2019)).

Fig. 4 provides evidence that our control scheme is real-time capable as the maximum execution time (including communication overhead) is always below the sampling time of 100 ms (black dashed line). Only in the first time step, i.e., when the distributed problem is initialized, the computation of a first (initial) solution takes longer than the sampling time, that is, 131 ms for the PAT (red). Initially, 9 ADMM iterations are required for convergence. However, the first time step can be viewed as an initialization phase which provides a viable initial guess for the second time step (in a receding horizon manner). During the rest of M-Step 1, we require 1 to 6 ADMM iterations for convergence while execution times for the PAT (red) and FAT (green) are mostly in a range of 50 ms to 70 ms — with a maximum of 87.5 ms at $t = 4.2 \text{ s}$ for the FAT (green). The SA (blue) shows lower execution times of 15 ms to 50 ms . During M-Step 2, consensus can be accomplished in a single ADMM step as the original minimum headway distance constraint (8g) is always satisfied. Thus, computation times are much lower, that is, these are in a range

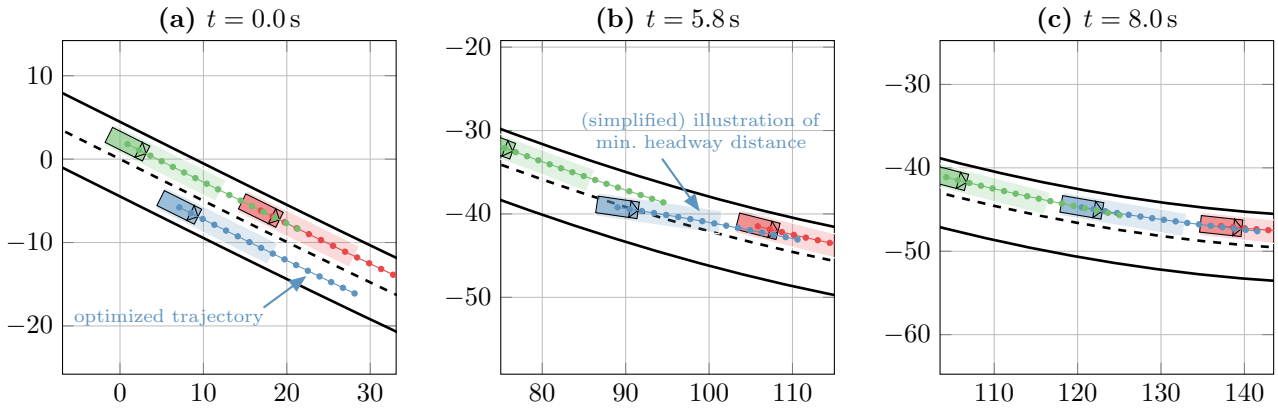


Fig. 5. Snapshots: (Left) Initial configuration: SA (blue) intends to change lanes; (Middle) SA (blue) changes lanes after required headway has been established (M-Step 2); (Right) SA (blue) has accomplished lane change maneuver.

of 4 ms to 7 ms. Only the SA (blue) temporarily requires 49 ms to solve its local OCP when the lateral acceleration constraints become active.

6. CONCLUSION AND FUTURE WORK

We have introduced a distributed control concept for fully automated lane change maneuvers of CAVs which is able to accommodate situations when the traffic is dense and the target lane is already occupied. To this end, we have embedded the nonconvex problem formulation in a consensus ADMM framework which has shown convincing performance and real-time capability in our simulation study. As part of future work, we intend to remove the central coordinator from the control scheme, to validate the scheme in experiments and to embed it into a broader motion planning framework.

REFERENCES

- 3GPP.org (2019). Enhancement of 3GPP support for V2X scenarios. 3GPP TS 22.186, V16.2.0. URL <https://portal.3gpp.org/desktopmodules/Specifications/SpecificationDetails.aspx?specificationId=3180>.
- An, H. and Jung, J. (2018). Design of a cooperative lane change protocol for a connected and automated vehicle based on an estimation of the communication delay. *Sensors*, 18(10).
- Bertsekas, D. and Tsitsiklis, J. (1989). *Parallel and Distributed Computation: Numerical Methods*. Prentice Hall.
- Bevilacqua, D., Cao, X., Gordon, M., Ozbilgin, G., Kari, D., Nelson, B., Woodruff, J., Barth, M., Murray, C., Kurt, A., Redmill, K., and Ozguner, U. (2016). Lane Change and Merge Maneuvers for Connected and Automated Vehicles: A Survey. *IEEE Transactions on Intelligent Vehicles*, 1(1), 105–120.
- Blasi, S., Kögel, M., and Findeisen, R. (2018). Distributed Model Predictive Control Using Cooperative Contract Options. *IFAC Conference on Nonlinear Model Predictive Control*, 51(20), 448–454.
- Bock, H. and Plitt, K. (1984). A Multiple Shooting Algorithm for Direct Solution of Optimal Control Problems. *IFAC World Congress*, 17(2), 1603–1608.
- Boyd, S., Parikh, N., Chu, E., Peleato, B., and Eckstein, J. (2011). Distributed Optimization and Statistical Learning via the Alternating Direction Method of Multipliers. *Found. and Trends in Machine Learning*, 3(1), 1–122.
- Hong, M., Luo, Z.Q., and Razaviyayn, M. (2016). Convergence Analysis of Alternating Direction Method of Multipliers for a Family of Nonconvex Problems. In *SIAM Journal on Optimization*, volume 26, 337–364.
- Hu, X. and Sun, J. (2019). Trajectory optimization of connected and autonomous vehicles at a multilane freeway merging area. *Transportation Research Part C: Emerging Technologies*, 101, 111–125.
- Katriniok, A., Sopasakis, P., Schuurmans, M., and Patrinos, P. (2019). Nonlinear Model Predictive Control for Distributed Motion Planning in Road Intersections Using PANOC. In *IEEE Conference on Decision and Control*, 5272–5278.
- Liu, P., Ozguner, U., and Zhang, Y. (2017). Distributed MPC for cooperative highway driving and energy-economy validation via microscopic simulations. *Transportation Research Part C: Emerging Techn.*, 77, 80–95.
- Nocedal, J. and Wright, S.J. (2006). *Numerical Optimization*. Springer, 2nd edition.
- Qian, X., de La Fortelle, A., and Moutarde, F. (2016). A hierarchical Model Predictive Control framework for on-road formation control of autonomous vehicles. In *IEEE Intelligent Vehicles Symposium*, 376–381.
- Rajamani, R. (2012). *Vehicle Dynamics and Control*, volume 2. Springer.
- Sopasakis, P., Fresk, E., and Patrinos, P. (2020). OpEn: Code Generation for Embedded Nonconvex Optimization. In *IFAC World Congress*.
- Stella, L., Themelis, A., Sopasakis, P., and Patrinos, P. (2017). A simple and efficient algorithm for nonlinear model predictive control. In *IEEE Conference on Decision and Control*, 1939–1944.
- Wang, D., Hu, M., Wang, Y., Wang, J., Qin, H., and Bian, Y. (2016). Model predictive control-based cooperative lane change strategy for improving traffic flow. *Advances in Mechanical Engineering*, 8(2), 1–17.
- Wang, Y., Yin, W., and Zeng, J. (2019). Global Convergence of ADMM in Nonconvex Nonsmooth Optimization. *Journal of Scientific Computing*, 78(1), 29–63.
- Wang, Z., Wu, G., and Barth, M. (2017). Developing a Distributed Consensus-Based Cooperative Adaptive Cruise Control System for Heterogeneous Vehicles with Predecessor Following Topology. *Journal of Advanced Transportation*.